Progress In Electromagnetics Research Letters, Vol. 33, 1–12, 2012

A DUALBAND METAMATERIAL ABSORBER BASED WITH RESONANT-MAGNETIC STRUCTURES

H.-M. Lee* **and H.-S. Lee**

Department of Electronic Engineering, Kyonggi University, Suwon, Republic of Korea

Abstract—In this paper, we present a new type of a double-negative metamaterial (MTM) absorber based with resonant-magnetic structures, with a periodic array composed of a split-ring resonator (SRR) and two open complementary split-ring resonators (OCSRRs). In contrast to common absorber configurations, the absorber proposed in this paper does not use a metallic back plate or a resistive sheet. In order to eliminate the need for this metallic back plate, a planar array of SRRs is placed parallel to the incident wave propagation direction. An appropriately designed combination structure of two OCSRRs and a SRR exhibits negative permittivity and negative permeability in the same frequency band. Each unit cell is printed on both sides of an FR-4 substrate. A prototype absorber was fabricated with a planar array of 75×42 unit cells. Both simulations and experiments verify the effectiveness of the proposed backplane-less MTM absorber. The proposed backplane-less absorber can be used for microwave applications.

1. INTRODUCTION

Microwave absorbers are used in military applications to reduce the radar cross-section (RCS) of a conducting object and the electromagnetic (EM) interference among microwave components. One of the earliest approaches to the design of EM absorber structures was based on the use of a Salisbury screen [1]. This type of absorber involves the use of a resistive sheet and a metallic ground plane to cancel out reflections from the screen. Recently, absorber technology has seen several advancements with the use of artificially structured metamaterials (MTMs) for creating a high-performance absorber for

Received 1 May 2012, Accepted 7 June 2012, Scheduled 20 June 2012

* Corresponding author: Hong-Min Lee (hmlee@kyonggi.ac.kr).

the microwave and terahertz frequency regimes [2–4]. According to the effective medium theory, MTMs can be represented by the complex values of electric permittivity $\varepsilon_{eff}(= \varepsilon' + j\varepsilon'')$ and magnetic permeability $\mu_{eff}(= \mu' + j\mu'')$. This permittivity and permeability can be independently controlled by varying the dimensions of the electric and magnetic components. Additionally, by tuning the electric and magnetic resonances, an MTM can be impedance-matched to free space. As a result, 100% absorbance is theoretically possible. Typically, absorbers contain metallic backing plates [5–8] for avoiding power transmission through the absorbers, which may be disadvantageous in stealth applications. In order to eliminate the use of metallic backing plates in absorbers, multiple split-ring resonator (SRR) bases with resonant-magnetic inclusion can be employed [9]. In addition, the absorber requires a resistive sheet placed at a certain distance from the MTM slab in order to match the impedance of free space. In this work, we present a compact absorber for low microwave frequencies by employing properly arrayed double-negative MTM unit cells, an arrangement that does not involve a metallic back plate or a resistive sheet. We have constructed an MTM unit cell employing an open complementary split-ring resonator (OCSRR) [10] and an SRR arrangement. The resonance frequency of the OCSRR is half that of a CSRR with identical dimensions. The OCSRR is a modified CSRR structure that exhibits negative permittivity, and the SRR structure itself exhibits negative permeability. We use a double-layered structure with an SRR and two OCSRRs placed on top of each other to construct a miniaturised MTM absorber unit cell for the 2–3 GHz frequency band.

2. DOUBLE-NEGATIVE UNIT CELL DESIGN

The configuration of the metallic backplane-less absorber with double-negative MTM unit cell structures is shown in Figure 1. The two metallic pattern layers separated by a dielectric spacer can be placed either orthogonal to the electromagnetic (EM) wave propagation direction or parallel to it. In the case where these layers are orthogonal to the EM wave propagation direction, as shown in Figure 1(a), the RCS of the object may increase at frequencies other than the frequency bands targeted in the design process. In order to avoid this problem, the metallic pattern layers should be placed parallel to the EM wave propagation direction, as shown in Figure 1(b). In principle, the SRR is employed for magnetic response. When a time-varying magnetic field, polarised normal to the plane of the SRR, is incident upon it, circulating currents are induced within the ring metallic patterns, resulting in a magnetic response.

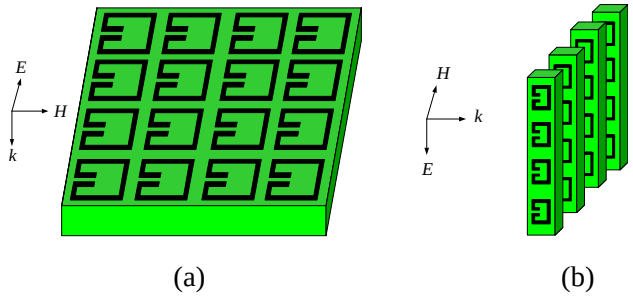

Figure 1. Sketch describing the structures of MTM absorber unit cell: (a) metallic patterns placed orthogonal to propagation direction k and (b) metallic patterns placed parallel to propagation direction k.

However, if the EM waves are incident normal to the planar SRR structure with the magnetic field completely perpendicular to the plane of the SRR and the electric field parallel to the gap of the SRR, as shown in Figure 1(b), an electromagnetic response is excited. This type of EM field orientation exhibits a much wider stop bandwidth [11]. A single unit cell of the proposed absorber consists of distinct metallic elements, as shown in Figures 2(a) and (b). The magnetic responses are provided by an SRR, as shown in Figure 2(a). The electric responses are provided by two symmetrically placed OCSRRs, as shown in Figure 2(b). We created a double-negative MTM structure by combining the OCSRRs with the SRR in a parallel plane, separated by a dielectric substrate, as shown in Figure 2(c). In order to achieve a dual-resonant frequency bands operation, two OCSRRs were placed symmetrically in the same dielectric plane. The absorber unit cell is made with an FR-4 substrate, which has a relative dielectric constant $\varepsilon_r = 4.6$, a loss tangent $\delta = 0.025$, and a thickness $t = 1.6\,\text{mm}$. The metal used for the metallic patterns is copper with a conductivity $\sigma = 5.8 \times 10^7\,\text{S/m}$. The geometrical dimensions of the proposed unit cell are: $a = 6\,\text{mm}$, $b = 7.2\,\text{mm}$, $c = 0.2\,\text{mm}$, $d = 0.2\,\text{mm}$, $e = 2.6\,\text{mm}$, $f = 4.8\,\text{mm}$, $k = 0.2\,\text{mm}$, $w = 0.4\,\text{mm}$ and $h = 6.8\,\text{mm}$. Computer simulations for one unit cell are carried out using the commercial solver Microwave Studio by CST. The program simulated a single unit cell with appropriate periodic boundary conditions. In Figure 2(c), the geometrical dimensions of the simulated unit cell in the y-direction are: $g/2 = 1.5\,\text{mm}$ and $t = 1.6\,\text{mm}$.

Perfect electric conductor boundary conditions are applied to the top and bottom walls of the waveguide, while perfect magnetic conductor boundary conditions are applied to the side walls of the

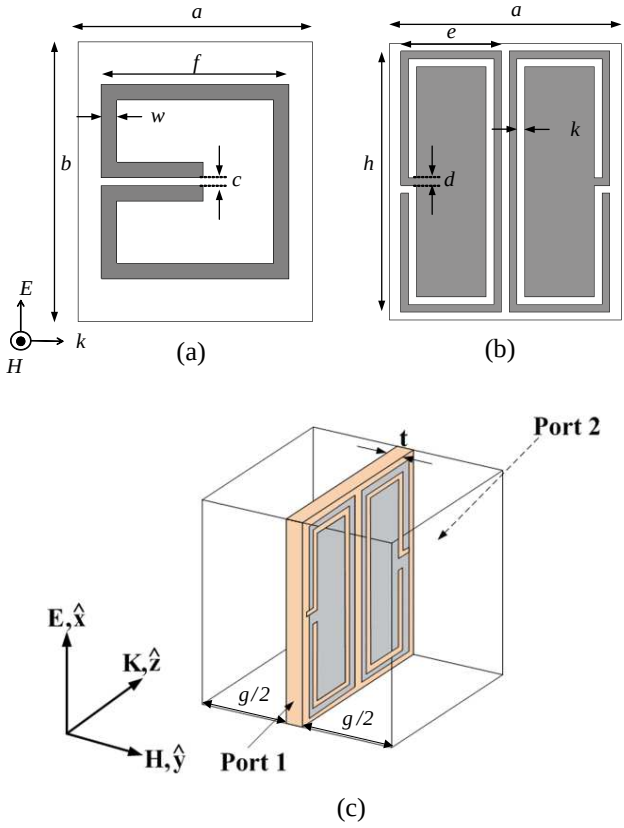

Figure 2. Geometry of the optimum absorber unit cell: (a) SRR and (b) OCSRRs. (c) Single unit cell showing the direction of propagation of incident electromagnetic wave.

waveguide. A single unit cell is placed inside a waveguide, and a vertically polarised transverse electromagnetic (TEM) wave is incident normally on the front side of port 1, as shown in Figure 2(c).

The scattering parameters of this MTM unit cell were then simulated, and the absorption was calculated using the equation $A = 1 - |S_{11}|^2 - |S_{21}|^2$. The simulated magnitudes of the S_{11} and S_{21} parameters are plotted in Figure 3. We observe that magnitudes of both the reflection and transmission coefficients are very low at the resonant frequencies of 2.95 GHz and 3.60 GHz, which indicates strong absorption of the EM wave energy. In order to express the effective permittivity and permeability of the artificial material in terms of scattering parameters, this information is conventionally

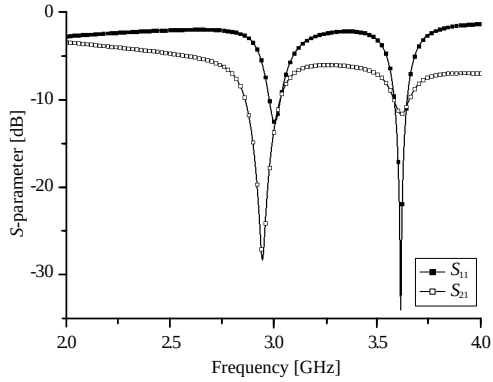

Figure 3. Amplitudes of the simulated S-parameters of the unit cell along the propagation direction.

retrieved from the scattering parameters of the unit cell under plane wave excitation [12]. The normalised intrinsic impedance X is defined by

$$X = \sqrt{\frac{\mu_r}{\varepsilon_r}} = \frac{1+\Gamma_{12}}{1-\Gamma_{12}}. \tag{1}$$

where Γ_{12} is given by

$$\Gamma_{12} = \frac{1-(S_{21}^2 - S_{11}^2)}{2S_{11}} \pm \sqrt{\left[\frac{1-\left(S_{21}^2 - S_{11}^2\right)}{2S_{11}}\right]^2 - 1}. \tag{2}$$

The appropriate sign is chosen so that $|\Gamma_{12}| \leqq 1$. The refractive index Y is also extracted as

$$Y = \sqrt{\varepsilon_r \mu_r} = j\frac{c_0}{d\omega}\left[\ln|z| + j\arg(z)\right], \tag{3}$$

where c_0 is the wave propagation velocity in free space, d the thickness of the dielectric substrate, ω the angular frequency, and z given by

$$z = \frac{(S_{11}+S_{21}) - \Gamma_{12}}{1-(S_{11}+S_{21})\Gamma_{12}}. \tag{4}$$

The effective permittivity ε_{eff} and permeability μ_{eff} can then be easily calculated from (1) and (3) as

$$\varepsilon_{eff} = Y/X \tag{5}$$

$$\mu_{eff} = XY. \tag{6}$$

The extracted effective refractive index and normalised intrinsic impedance of the proposed absorber over a frequency range of 2.2–4.0 GHz are plotted in Figure 4.

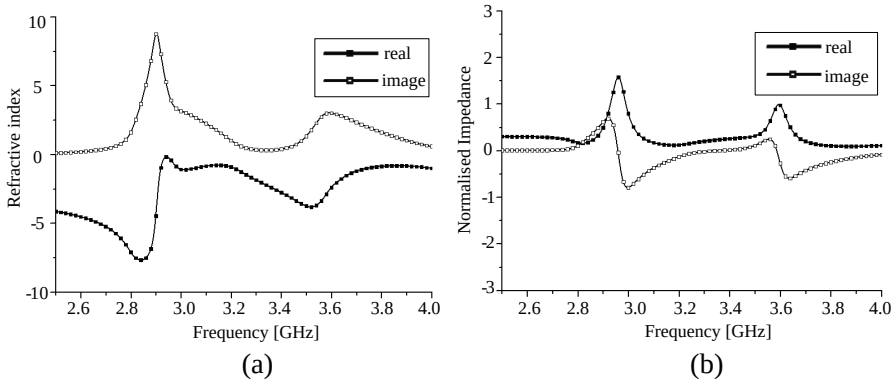

Figure 4. (a) Extracted effective refractive index and (b) normalised intrinsic impedance.

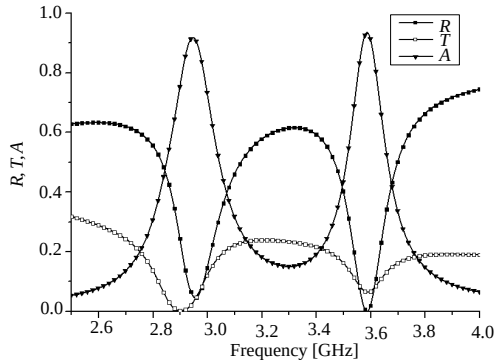

Figure 5. Simulation results for the MTM absorber: absorption $A(\omega)$, reflectance $R(\omega)$ and transmission $T(\omega)$.

As shown in Figure 4(a), the unit cell has a negative real part of the refractive index near its resonant frequencies of 2.95 GHz and 3.60 GHz. The negative sign of the real part of refractive index gives the phase velocity direction for left-handed (LH) medium [13]. The imaginary part of the refractive index shows a maximum positive value near these frequencies ($n'' \approx 8$, and 2.2), which indicates strong absorption of the EM wave energy. As a result, the proposed structure functions as a dual-band MTM absorber. In addition, it can be observed that impedance is well matched at resonant frequencies. In Figure 5, we show the simulation results for the proposed MTM absorber, through

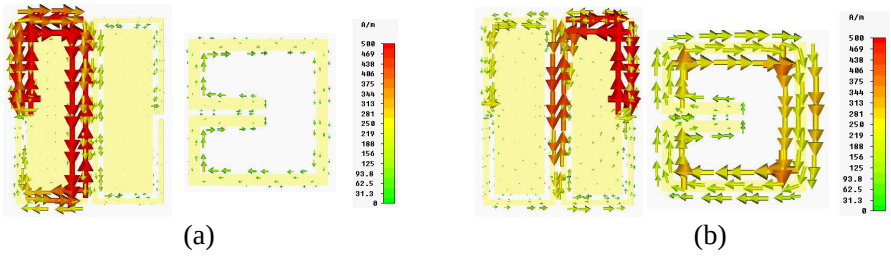

Figure 6. Simulated current distributions of the proposed absorber unit cell at (a) 2.95 GHz and (b) 3.60 GHz.

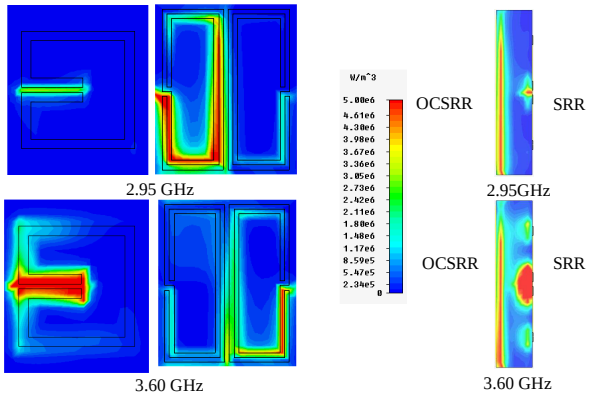

Figure 7. The top and side plane views of the simulated average power loss densities of the absorber unit cell at two resonant frequencies.

the plotting of absorption $A(\omega)$, reflectance $R(\omega)$, and transmission $T(\omega)$. It can be observed that the reflectance and transmission of the absorber sharply reduce to a minimum at both frequencies, 2.95 GHz and 3.60 GHz, which also show two distinct absorption peaks of 92% and 94%, respectively. The nature of this absorption can be understood from Figures 6 and 7, which show the simulated surface current densities and the power loss densities, respectively, in the top and bottom resonator structures at 2.95 GHz and 3.60 GHz. As shown in Figure 6, at the two resonance frequencies, the counter-circulating current flow on the SRR provides magnetic resonance, and a stronger current density occurs in the shorted-end gap of the OCSRRs. For the resonance at 2.95 GHz, the power loss is concentrated strongly in the vicinity of the open gaps of the OCSRRs; this power loss is stronger than that in the gap of the SRR, as shown in Figure 7(a).

In contrast, for the resonance at 3.60 GHz, the power loss mainly

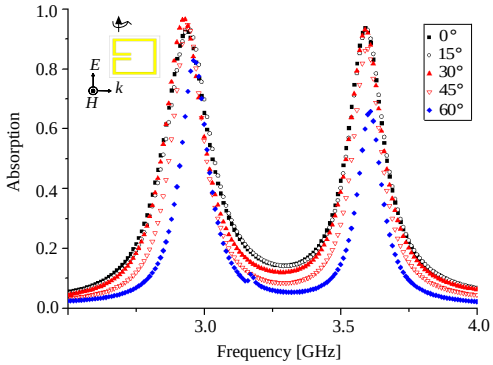

Figure 8. Simulated absorption values at different oblique incident angles.

occurs in the space neighbouring the gaps of the SRR this power loss is stronger than the gap of the OCSRRs, as shown in Figure 7(b). These results indicate that the absorption does not homogeneously occur in the MTM unit cell. It is found that strong absorption can occur in the gaps of the SRR and OCSRRs. For the resonance at 2.95 GHz, the OCSRR placed on the left side mainly contributes to the EM energy absorption and the SRR acts as an impedance matching element. In addition, for the resonance at 3.60 GHz, the SRR mainly contributes to the EM energy absorption and the OCSRRs acts as an impedance matching element. As a result, the proposed absorber acts as a dual-band absorber. The simulated absorption curve for the different incident angles of EM waves over a broad frequency range is plotted in Figure 8. It is observed from Figure 8 that as the incidence angles increase, the absorption bandwidth decreases slightly for both the low- and high-frequency absorption bands. For an incident angle of 60°, the peak absorption drops to 82% at the low-frequency absorption band and 67% at the high-frequency absorption band. This can be explained by the fact that the incident magnetic field can no longer effectively induce resonant currents on the metallic patterns on the SRR and OCSRRs.

3. EXPERIMENTAL RESULT

We fabricated a prototype absorber for experimentation. Photographs of the fabricated two-layer metallisation MTM absorber sample are shown in Figure 9. The sample was etched on an FR-4 substrate (relative dielectric constant $\varepsilon_r = 4.6$, loss tangent $\delta = 0.025$, and

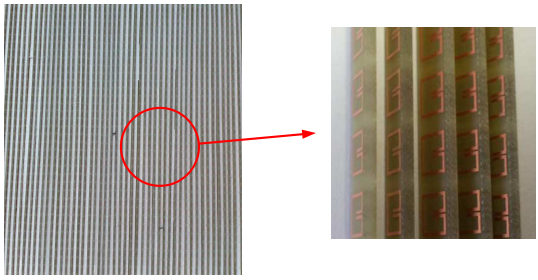

Figure 9. (a) Photographs of the fabricated prototype absorber with the stacked array of absorber strips. A polystyrene foam substrate with a relative permittivity of 1.02 is inserted between absorber strips. (b) Single absorber strips made with SRR and OCSRRs configuration are aligned vertically parallel to the wave propagation direction.

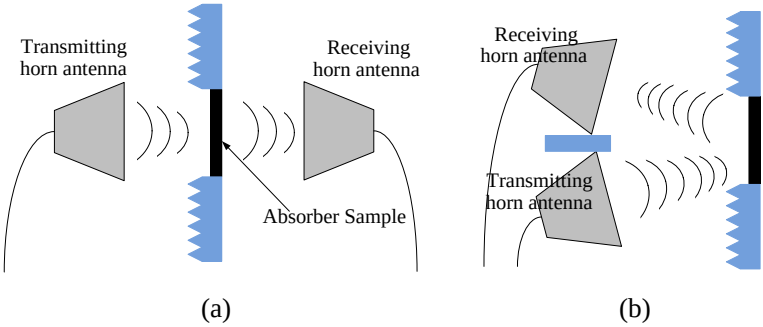

Figure 10. (a) Schematics of reflection and transmission measurement test set up for normal incidence and (b) oblique incidence.

thickness $t = 1.6\,\text{mm}$) using standard photolithography techniques. In order to verify the effectiveness of the double-negative MTM absorber cells without a metallic backing plate, a planar array of absorber unit cells (75×42) was mounted on an acryl substrate frame.

One period of the absorber strip consists of 42 unit cells etched on both sides of an FR-4 substrate. The inter-element spacing between the two absorber strips was set to 3 mm, and the total size of the planar absorber was $301 \times 305\,\text{mm}$.

We experimentally verified the behaviour of the absorber by measuring the S-parameters of a planar array of unit cells. Figure 10 shows the schematic of the test set-up for reflection and transmission

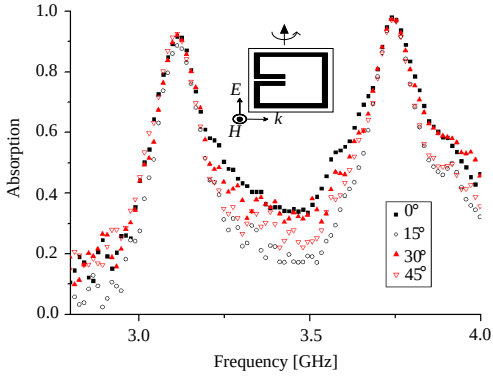

Figure 11. Measured absorption values at different oblique incident angles.

measurement of the fabricated absorber sample. We used a vector network analyser and two R-band microwave horn antennas. Measurements were taken over a frequency range from 2.6 to 4.0 GHz. As shown in Figure 10(a), a pair of horn antennas was used to transmit the EM wave on the sample absorber sheet and receive both the reflected and transmitted signals to obtain the absorption for normal incidence. Microwave absorbing material is placed between horns and surrounding the sample sheet to eliminate unwanted edge scattering. The height of the horn antennas is maintained at 1.2 m and the distance between horns and sample sheet is 0.5 m to eliminate near-field coupling effects. To test the absorption properties for oblique incidence angles, two horns were focused on the sample sheet on the same side, as shown in Figure 10(b). The sample sheet was rotated from 0° to 50° with 15° angle steps for the measurement of the absorption properties for oblique incidence angles. The calculated absorption using measured magnitudes of the S_{11} and S_{21} parameters for the planar arrayed unit cells are plotted in Figure 11.

The results show that the backplane-less planar absorber structure acts as a dual-band absorber. However, the experimental peak absorption frequencies are shifted approximately 80 MHz higher when compared to the simulated results. The proposed absorber shows a absorption peak over 92% and 94% at 3.13 GHz and 3.73 GHz, respectively. The proposed planar absorber structure shows the possibility of a planar-type absorber without metallic backing plates or a resistive sheet.

4. CONCLUSIONS

A new type of a backplane-less planar-type microwave absorber based on arrayed double-negative MTM unit cells was presented. We have shown that properly arrayed single unit cells with an SRR and two OCSRRs can effectively absorb most of the incident power. The main advantage of the proposed absorber is the absence of a metallic back plate or a resistive sheet The total miniaturised MTM absorber unit cell size was $6 \times 7.2 \times 1.6$ mm. The substrate thickness of the proposed metamaterial absorber is about $0.016\lambda_0$ (1.6 mm at 3 GHz) and the absorber thickness in the EM wave propagation direction has shown to lead $0.06\lambda_0$ (the unit cell width $a = 6$ mm). If we designed an absorber unit cell composed of an SRR and an OCSRR for single-band operation, the absorber-electrical thickness can be reduced to $0.03\lambda_0$. Through numerical simulation and calculation, the effective parameters of the proposed double-negative MTM unit cell have been extracted. The performance of the proposed absorber was experimentally verified. This structure serves as a dual-band absorber in the microwave frequency region. The proposed layout can be easily extended to work for more compact, thinner backplane-less planar absorber designs for millimetre and terahertz frequency applications.

ACKNOWLEDGMENT

This research was supported Basic Science Research Program through National Research Foundation of Korea (NRF) funded by the Ministry of Education, Science and Technology (No. 2010-0011646).

REFERENCES

1. Fnate, R. L. and M. T. McCormack, "Reflection properties of the Salisbury screen," *IEEE Trans. Antennas Propag.*, Vol. 30, 1443–1454, 1968.
2. Landy, N. I., S. Sajuyigbe, J. J. Mock, D. R. Smith, and W. J. Padilla, "Perfect metamaterial absorber," *Phys. Rev. Lett.,* 274021–274024, 2008.
3. Tao, H., N. I. Landy, C. M. Bingham, X. Zang, R. D. Averitt, and W. J. Padilla, "A metamaterial absorber for the terahertz regime: Design, fabrication and characterization," *Opt. Express*, Vol. 16, 7181–7188, 2008.
4. Cheng, Y. and H. Yang, "Design, simulation, and measurement of metamaterial absorber," *Microwave Opt. Tech. Lett.*, Vol. 52, 877–880, 2010.

5. Tao, H., C. M. Bingham, D. Pilon, K. Fan, A. C. Strkwerda, D. Shrekenhammer, W. J. Padilla, X. Zhang, and R. D. Averitt, "A dual band terahertz metamaterial absorber," *J. Appl. Phys. D*, Vol. 43, 225102–225106, 2010.
6. Li, M.-H., H.-L. Yang, and X.-W. Hou, "Perfect metamaterial absorber with dual bands," *Progress In Electromagnetics Research*, Vol. 108, 37–49, 2010.
7. Lee, J. and S. Lim, "Bandwidth-enhanced and polarization-insensitive metamaterial absorber using double resonance," *Electron. Lett.*, Vol. 47, 8–9, 2011.
8. Cheng, Y., H. Yang, Z. Cheng, and N. Wu, "Perfect metamaterial absorber based on a split-ring-cross resonator," *J. Appl. Phys. A*, Vol. 102, 99–103, 2010.
9. Alici, K. B., F. Bilotti, L. Vegni, and E. Ozbay, "Experimental verification of metamaterial based subwavelength microwave absorbers," *J. Appl. Phys.*, Vol. 108, 0831131–0831136, 2010.
10. Velez, A., F. Aznar, J. Bonache, J. M. Velazquez-Ahumada, and F. Martin, "Open complimentary split ring resonators (OCSRRs) and their application to wideband CPW band pass filters," *IEEE Microwave & Wirel. Compon. Lett.*, Vol. 19, 197–199, 2009.
11. Katsarakis, N., T. Koschny, and M. Kafesaki, "Electric coupling to the magnetic resonance of split ring resonators," *Appl. Phys. Lett.,* Vol. 84, No. 15, 2943–2945, 2004.
12. Nicolson, A. M. and G. F. Ross, "Measurement of the intrinsic properties of materials by time-domain technique," *IEEE Trans on Instrumentation and Measurement,* Vol. 19, No. 4, 377–382, 1970.
13. Depine, R. A. and A. Lakhtakia, "A new condition to identify isotropic dielectric-magnetic materials displaying negative phase velocity," *Microwave Opt. Tech. Lett.*, Vol. 41, 315–316, 2004.